

## CHAPTER 3

### FRACTURE MECHANICS

Fatigue and fracture of materials is a well accepted science and a large number of references cover the basics <sup>[T6,T10,T11,T12,T13,T14]</sup>. Fracture mechanics generally deals with the analysis of structures with cracks or sharp notches that result in numerical discontinuities in the linear elastic strain field.

In practice, the discontinuities are relieved by plastic material behaviour in a region around the crack front. Fracture mechanics applications are subdivided in a number of approaches depending on the amount of plasticity that occurs at the crack front.

Linear elastic fracture mechanics (LEFM) assumes small scale yielding so that the surrounding elastic body dominates the strain field in the region of the crack front. It follows that the strain solution of the surrounding elastic body can be extrapolated to the crack front to give single valued solutions from which ruling parameters can be derived, so as to describe the crack front characteristics. LEFM is applicable to most heavy sectioned, low temperature structural components. The J-parameter, as is used in elastic-plastic fracture mechanics is equivalent to the K-parameter approach for the linear elastic case.

The ruling parameters in fracture mechanics are dependent on geometry, applied stress and material properties. A large compendium of empirical solutions is available for specific cases, but in general the fracture parameters must be calculated from continuum mechanics principles. Analytical solutions are limited because of the complexity of the boundary value problem in continuum mechanics.

### 3.1 GENERAL PRINCIPLES

The ruling parameters in LEFM are stress intensity factors for the different modes of loading namely mode I, II and III. Figure 3.1 shows a graphical presentation of the three modes. Each mode has an associated stress intensity i.e.  $K_I$ ,  $K_{II}$  and  $K_{III}$ .

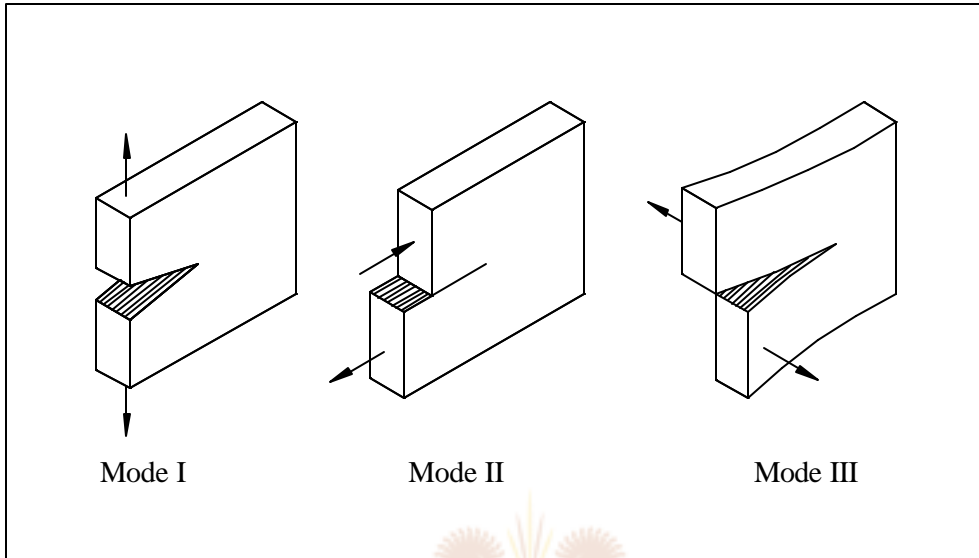


Figure 3.1. Fracture modes

This chapter deals with the theoretical development of LEFM and methods of calculating the stress intensity factors.

#### 3.1.1 Griffith Theory <sup>[T12]</sup>

Griffith performed the first analysis attempts on components with sharp discontinuities. The theory was developed from applications to ideally brittle materials like glass and is based on an energy criterion. An infinite centre cracked panel, as shown in figure 2.3, with a uniaxial tension of  $\sigma$  perpendicular to a crack with a length of  $2a$  is considered.

Conservation of energy demands that the work done on a body by external forces,  $F$ , is not lost but conserved as strain energy,  $U$ , in the case of linear elastic solids (no heat generated etc. due to plastic deformation). The relationship is

$$F - U = 0 \tag{3.1.1}$$

Consider a plate of unit thickness as depicted in figure 3.2. The work due to external loads are written as

$$F = \frac{1}{2} P \delta = \frac{1}{2} (\sigma A) \left( \frac{\sigma}{E} L \right) = \frac{1}{2} \frac{\sigma^2}{E} AL \quad (3.1.2)$$

where  $A$  is the cross sectional area. The strain energy for linear elasticity is given per unit volume in equation 2.1.36. The total strain energy is expressed as

$$U = \frac{1}{2} \sigma \epsilon V = \frac{1}{2} \frac{\sigma^2}{E} AL \quad (3.1.3)$$

where  $V$  is the volume. Substituting 3.1.2 and 3.1.3 in 3.1.1 indicates that

$$U = \frac{1}{2} P \delta \quad (3.1.4)$$

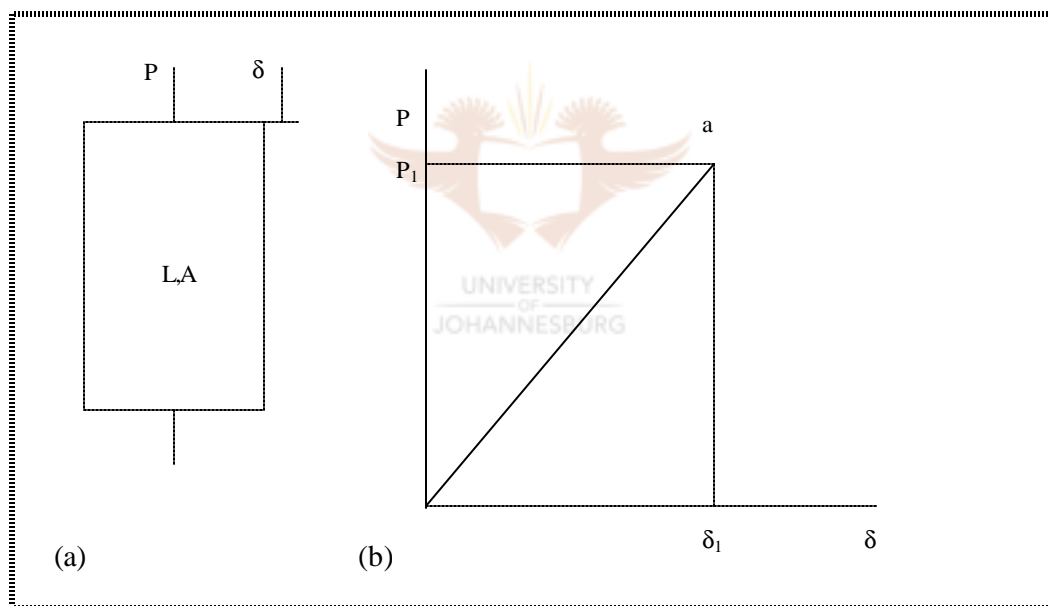


Figure 3.2: Energy release during constant load. (a) Plate of length,  $L$ , and area,  $A$ , subjected to a load,  $P$ , and corresponding displacement,  $\delta$ . (b) Load displacement record.

Equations 3.1.1 to 3.1.4 must hold for the same body with a crack of length  $2a$  as indicated in figure 3.3. If the crack is extended to a length of  $2(a+da)$ , less load will be required to cause the same displacement, as the stiffness is less, or alternatively the displacement will increase if the load remains constant.

A third term, namely the work expended in fracturing the material over  $da$  (denoted  $W$ ), must be incorporated into equation 3.1.1 since energy must still be conserved. The conservation equation, 3.1.1, now only covers changes in energy

$$\frac{d}{da}(F - U) = \frac{dW}{da} \quad (3.1.5)$$

Examining figure 3.3, it is noted that the load,  $P_1$ , does work,  $F = P_1(\delta_2 - \delta_1)$  during the crack extension. The strain energy, calculated by 3.1.4, increases from  $\frac{1}{2}P_1\delta_1$  to  $\frac{1}{2}P_1\delta_2$ . Equation 3.1.5 becomes

$$P_1(\delta_2 - \delta_1) - \frac{1}{2}P_1(\delta_2 - \delta_1) = \frac{1}{2}P_1(\delta_2 - \delta_1) = \frac{dW}{da} \quad (3.1.6)$$

It was derived, in a similar manner, that the deliverable energy is the same for a case of incremental crack growth under constant displacement and that it is always equal to the change in strain energy as expressed in equation 3.1.6.

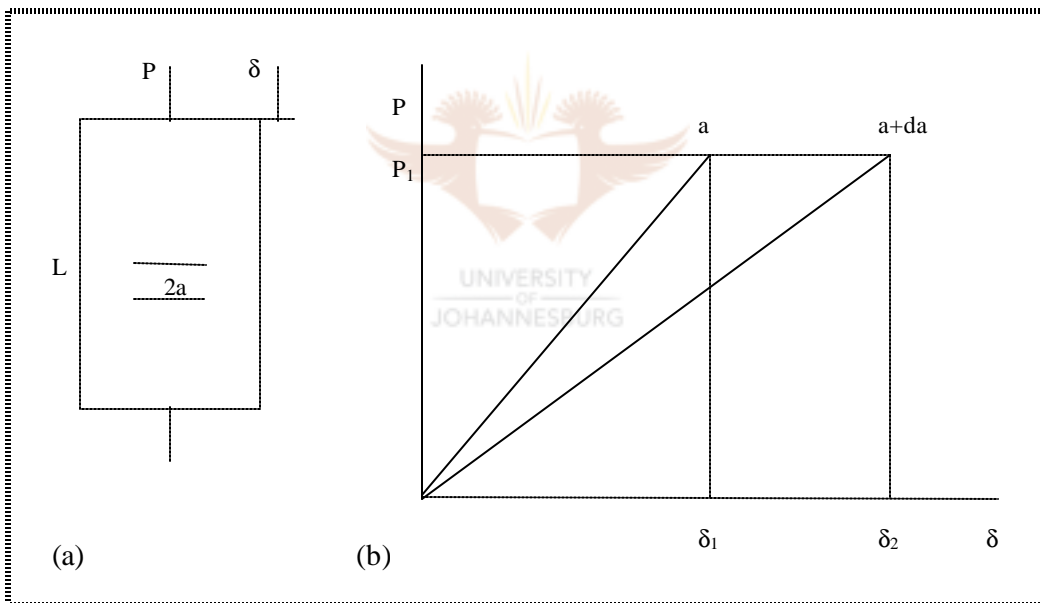


**Figure 3.3: Energy release during constant load. (a) Plate of length,  $L$ , with a crack of length,  $2a$ , subjected to a load,  $P$ , and corresponding displacement,  $\delta$ . (b) Load displacement record for an incremental crack extension of  $da$ .**

The net change in strain energy was evaluated by Buekner <sup>[T13]</sup> who realised that the strain energy due to a finite crack in an infinite plate subjected to a stress,  $\sigma$ , at infinity as in figure 2.3, is equal to the work done by a stress of equal magnitude but opposite sign, acting on the crack face i.e. the release of the stress on the crack face over the distance of the crack face displacement.

This gives, for plane strain,

$$\begin{aligned} F - U &= 2 \int_0^a \frac{1}{2} \sigma u_2(x_1) dx_1 = \frac{2(1-\nu^2)\sigma^2}{E} \int_0^a \sqrt{(a^2 - x_1^2)} dx_1 \\ &= \frac{2(1-\nu^2)\sigma^2}{E} \left( \frac{a^2 \pi}{2 \cdot 2} \right) = \frac{(1-\nu^2)\pi a^2 \sigma^2}{2E} \end{aligned} \quad (3.1.7)$$

with  $u_2$  as derived in equation 2.4.16. Differentiating 3.1.7 with respect to  $a$  gives

$$\frac{\partial F}{\partial a} - \frac{\partial U}{\partial a} = \frac{\partial W}{\partial a} = G = \frac{(1-\nu^2)\sigma^2 \pi a}{E} \quad (3.1.8)$$

with the crack driving force, also the strain energy release rate, denoted as  $G$  in honour of Griffith whose original formula had the same form giving  $G$  as the surface energy.  $G$  includes the surface energy and the plastic energy dissipation as proposed and used by Griffith. A fracture stress,  $\sigma_f$ , is calculated from 3.1.8, resulting in:

$$\sigma_f = \left( \frac{1}{\pi} \frac{EG}{(1-\nu^2)a} \right)^{\frac{1}{2}} \quad (3.1.9)$$

It was proven by Sneddon <sup>[P5]</sup> that displacement solutions for other (other than infinite centre cracked panel) result in the same form of equation as 3.1.9 and differ only by a numerical constant.

The assumption is made that the amount of energy required to create a unit area of new crack area by crack extension (fracture) is a material property denoted  $G_{IC}$ . Unstable crack growth will occur when  $G$ , as calculated by 3.1.8, reaches the critical material limit.

### 3.1.2. Stress Intensity Approach <sup>[T6,T10,T11,T12,T13,T14]</sup>

The stress intensity approach is developed from considerations with regard to the expression for stresses in the vicinity of the crack tip as approximated by equation 2.4.15 namely

$$\begin{aligned} \sigma_{ii} &= \sigma \sqrt{\frac{a}{2r}} f_{ij}(\theta) + \sum_n O \left[ \left( \frac{r}{a} \right)^n \right] \\ &= \frac{K}{\sqrt{2\pi r}} f_{ij}(\theta) + \dots \end{aligned} \quad (3.1.10)$$

showing the first term only. The quantity,  $K$ , in equation 3.1.10 is defined as

$$K_I = \sigma\sqrt{\pi a} \quad (3.1.11)$$

and is denoted  $K_I$  because the loading is of the mode I type.  $K_I$  is related to the energy balance parameter,  $G$ , derived in section 3.1.1 by examining equation 3.1.8 revealing, for plane strain, that

$$G = G_I = \frac{(1-\nu^2)K_I^2}{E} \quad (3.1.12)$$

A similar argument for mode II and III type load provides expressions as follows:

$$G_{II} = \frac{(1-\nu^2)K_{II}^2}{E} \quad (3.1.13)$$

$$G_{III} = (1+\nu)\frac{K_{III}^2}{E} \quad (3.1.14)$$

The total strain energy release rate is obtained by adding equations 3.1.12 to 3.1.14 to give:

$$G_{TOT} = \frac{(1-\nu^2)K_I^2}{E} + \frac{(1-\nu^2)K_{II}^2}{E} + (1+\nu)\frac{K_{III}^2}{E} \quad (3.1.15)$$

with  $K_{II} = \tau_{in\ plane}\sqrt{\pi a}$  (3.1.16)

$$K_{III} = \tau_{out\ of\ plane}\sqrt{\pi a} \quad (3.1.17)$$

and  $\tau$  denoting shear stress. Fracture occurs when  $G_{appl}$  exceeds a characteristic material limit, normally expressed as a limit in the stress intensity, where fracture occurs.

$$K_{eff} \geq K_{IC} \quad (3.3.3)$$

$K$  controlled fracture is described by Linear Elastic Fracture Mechanics (LEFM) where the plasticity at the crack tip is almost fully constrained by the surrounding elastic material. This topic is covered earlier in this chapter.

### 3.1.3 Linear Elastic Fracture Mechanics

If a body obeys the linear elastic stress-strain relationship, the stresses at the crack tip are given by equation 3.1.10. Close to the crack tip, where  $r$  is small, only the first term is significant so that the stress solution for this region is written as:

$$\sigma_{ij} = \frac{K_I}{\sqrt{2\pi r}} f_{ij}(\theta) \quad (3.1.18)$$

The remote stress, the crack length and body dimensions are the only factors influencing the stress. These factors will influence  $K$  in the same way as it influences  $\sigma$ . The region surrounding the crack tip where the first term of equation 3.1.18 describes the stress field to sufficient accuracy is called the  $K$ -dominant region. If the inelastic processes at the crack tip are entirely contained within the  $K$ -dominant region, the inelastic process is controlled by the deformation of the inelastic region surrounding it. Because this deformation is solely dependent on  $K$ , crack instability must be associated with a critical value of  $K$ .

These assumptions form the basis of linear elastic fracture mechanics. The validity is analysed by considering the radius of the inelastic region at the crack tip. The Von-Mises yield criterion states that the onset of yielding occurs when

$$s_Y \sqrt{2} = \sqrt{(s_{11} - s_{22})^2 + (s_{11} - s_{33})^2 + (s_{33} - s_{22})^2} \quad (3.1.19)$$

For plane strain the magnitude of the stresses at the crack tip are related as follows, in accordance with equation 2.4.15:

$$\left. \begin{aligned} \sigma_{11} &= \sigma_{22} = \sigma_c \\ \sigma_{33} &= \nu(\sigma_{11} + \sigma_{22}) = 2\nu\sigma_c \end{aligned} \right\} \quad (3.1.20)$$

If a Poisson ratio of 0.3 is considered, substitution of equation 3.1.20 into 3.1.19 indicates that yield at a crack tip in plane strain will only start occurring when the stress reaches approximately 3 times the yield stress i.e.  $\sigma_c = 3\sigma_Y$ .

An approximate crack tip plastic radius,  $r_p$ , can now be calculated assuming a remote stress equal to half the yield stress and calculating the stress according to equation 2.4.18.

$$3\sigma_Y = \frac{\sigma_Y}{2} \sqrt{\frac{a}{2r_p}} \quad (3.1.21)$$

This gives  $\frac{r_p}{a} = \frac{1}{72} = 0.014$ . For this case, a crack of 10 mm would have a plastic radius of 0.14 mm.

The K dominance around this ratio of r:a is investigated by considering the influence of the various terms of equation 2.4.12 in relation to the full solution of equation 2.4.10 as well as the K dominance approximation of equation 3.1.10.

The graph in figure 3.4 shows the stress solution at the crack tip for a unit remote stress as a function of r/a. The percentage error for the K dominant term is also shown.

Figure 3.4 indicates that the percentage error at the plastic radius, calculated earlier, is in the order of 0.5%. It must be realised that the deviation in other test pieces (other than infinite plate) will be slightly different, as their stress distributions are slightly different.

It was mentioned in the previous section that a material has a characteristic limit in stress intensity that it can absorb. This limit is called the material toughness and varies as a function of temperature and plane stress vs. plane strain conditions. The material toughness in plane strain is denoted  $K_{IC}$ . When this limit is exceeded, fracture occurs.

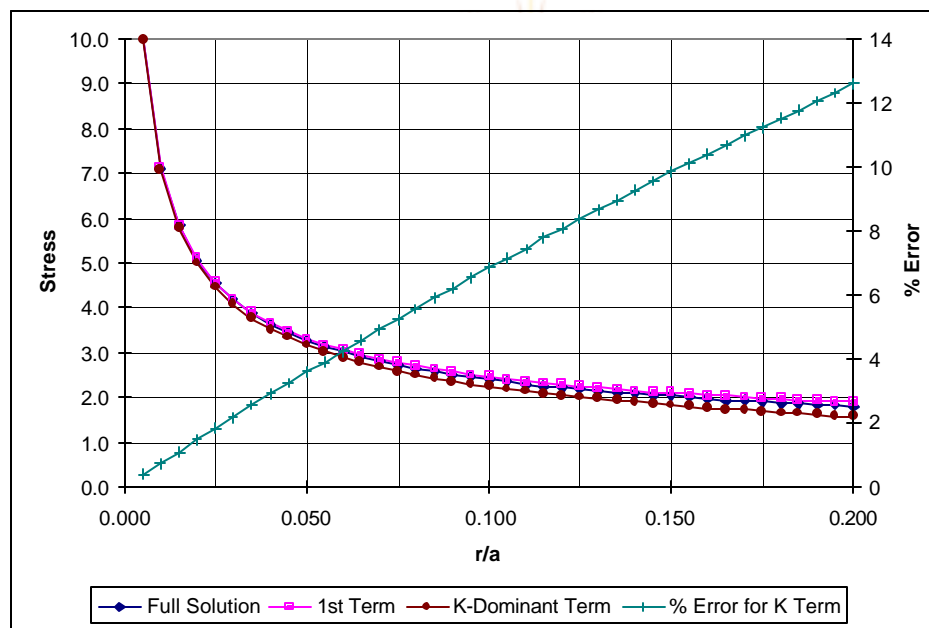


Figure 3.4 : Various approximations for stress distribution at the crack tip for a unit remote stress with stress in MPa and:

- Full Solution: Equation 2.4.10
- 1<sup>st</sup> Term: First term of equation 2.4.12
- K-Dominant term: First term of equation 3.1.10



### 3.2 CALCULATION OF STRESS INTENSITY [T6]

Equation 2.4.15 is written in polar co-ordinates as

$$\sigma_{rr} = \frac{K_I}{\sqrt{2\pi r}} \cos\left(\frac{\theta}{2}\right) \left(\frac{3}{2} - \frac{1}{2} \cos \theta\right) \quad (3.2.1.a)$$

$$\sigma_{\theta\theta} = \frac{K_I}{\sqrt{2\pi r}} \cos\left(\frac{\theta}{2}\right) \left(\frac{1}{2} + \frac{1}{2} \cos \theta\right) \quad (3.2.1.b)$$

omitting higher order terms. It is evident that equations 3.2.1 cannot be applied to the crack front because of the singularity. The constitutive law, equation 2.2.6, is applied to obtain the strain resulting in:

$$\mathbf{e}_{rr} = \frac{\int u_r}{\int r} = \frac{1-n^2}{E} \left( \mathbf{s}_{rr} - \frac{n}{1-n} \mathbf{s}_{qq} \right) \quad \text{and} \quad (3.2.2.a)$$

$$\mathbf{e}_{qq} = \frac{1}{r} \frac{\int u_q}{\int q} + \frac{u_r}{r} = \frac{1-n^2}{E} \left( \mathbf{s}_{qq} - \frac{n}{1-n} \mathbf{s}_{rr} \right) \quad (3.2.2.b)$$

The  $r^{-1}$  singularity will still apply to the stain, but after integration (applying compatibility equations 2.2.3) the displacement result would yield

$$u_r = \frac{2K_I r^{1/2} (1-n^2)}{\sqrt{2p} E} \left[ \frac{5-8n}{4(1-n)} \cos\left(\frac{q}{2}\right) - \frac{1}{4(1-n)} \cos\left(\frac{3q}{2}\right) \right] \quad (3.2.3.a)$$

$$u_q = \frac{K_I r^{1/2} (1-n^2)}{\sqrt{2p} E} \left[ \frac{8n-7}{2(1-n)} \sin\left(\frac{q}{2}\right) + \frac{1}{2(1-n)} \sin\left(\frac{3q}{2}\right) \right] \quad (3.2.3.b)$$

with and  $q$  and  $r$  as for figure 3.5 and assuming symmetry around the crack plane. Analysing equation 3.2.3 with  $q = \pi$  ( $u_1$  corresponding to displacement of the crack surface) gives

$$u_1 = \frac{K_I r^{1/2} (1-\nu^2)}{\sqrt{2\pi} E} \left[ \frac{8\nu-7}{2(1-\nu)} - \frac{1}{2(1-\nu)} \right] = -\frac{4K_I r^{1/2} (1-\nu^2)}{\sqrt{2\pi} E} \quad (3.2.4)$$

$K_I$  is evaluated at the crack tip from the displacement results of equation 3.2.4 as:

$$K_I = \lim_{r \rightarrow 0} \left( \frac{-u_c}{4} \frac{E}{(1-\nu^2)} \sqrt{\frac{2\pi}{r}} \right) \quad (3.2.5)$$

Equation 3.2.5 implies that if the displacement of the crack surface can be measured or calculated, the stress intensity can be calculated by extrapolation the ratio  $u/\sqrt{r}$  to the crack tip.

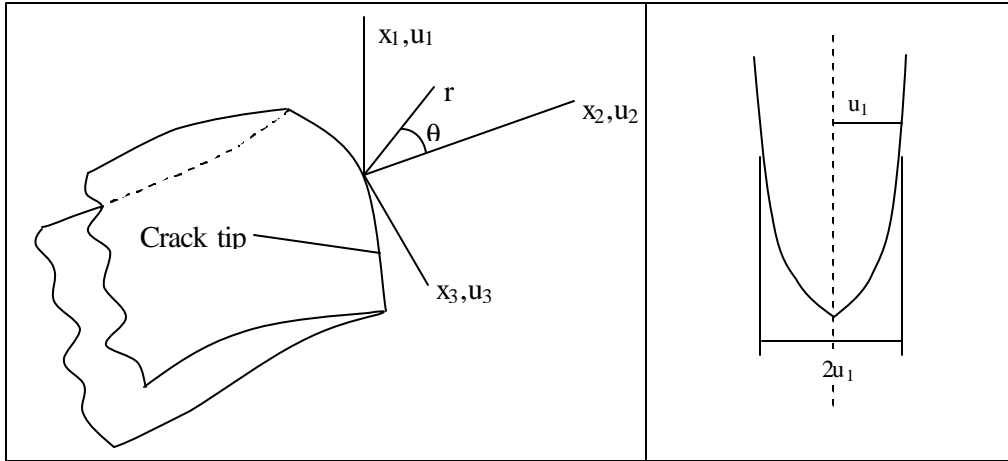


Figure 3.5: Displacements at crack tip

Similar treatment of  $u_2$  and  $u_3$  give the solutions to  $K_{II}$  and  $K_{III}$  so that for a full 3D crack model ( $u_i = 2u_{i,eq 3.2.5}$ ) the complete stress intensity solution is:

$$\left. \begin{aligned} K_I &= \lim_{r \rightarrow 0} \left( \frac{-\Delta u_1}{8} \frac{E}{(1-\nu^2)} \sqrt{\frac{2\pi}{r}} \right) \\ K_{II} &= \lim_{r \rightarrow 0} \left( \frac{-\Delta u_2}{8} \frac{E}{(1-\nu^2)} \sqrt{\frac{2\pi}{r}} \right) \\ K_{III} &= \lim_{r \rightarrow 0} \left( \frac{-\Delta u_3}{8} \frac{E}{(1-\nu^2)} \sqrt{\frac{2\pi}{r}} \right) \end{aligned} \right\} \quad (3.2.6)$$

with  $\Delta u_1$ ,  $\Delta u_2$  and  $\Delta u_3$  as the relative movement of one crack face to the other in the co-ordinate directions indicated by figure 3.5.

### 3.3 FATIGUE [T12,T14]

Fatigue crack initiation and growth occur when a component is subjected to a cyclic stress. Fatigue crack growth is governed by 3 stages as depicted in figure 36, which shows a schematic plot of crack growth rate,  $da/dN$ , vs. stress intensity range,  $\Delta K$ , on a log-log plot. At low  $\Delta K$ , stage I, crack growth is associated with threshold,  $\Delta K_{th}$ , effects. Crack growth will occur once the cyclic stress intensity reaches or exceeds the fatigue threshold of the material.

$$\Delta K_{app} \geq \Delta K_{th} \quad (3.3.1)$$

The stress intensity threshold is influenced by a large number of factors including:

- stress ratio, R
- mixed mode loading ( $K_{I,II,III}$ )
- material condition (grain size etc)
- environment (air, steam etc).

Once the applied stress intensity reaches the threshold value and the crack grows beyond the influence of threshold effects, stage II, the curve is essentially linear and is described by the Paris law as:

$$\frac{da}{dN} = C(\Delta K)^\alpha \quad (3.3.2)$$

The constants C and  $\alpha$  are material constants and are also influenced by the same variables as is the case for the threshold values. Crack growth will occur according to the Paris law until stage III is reached where rapid, unstable crack propagation takes place.

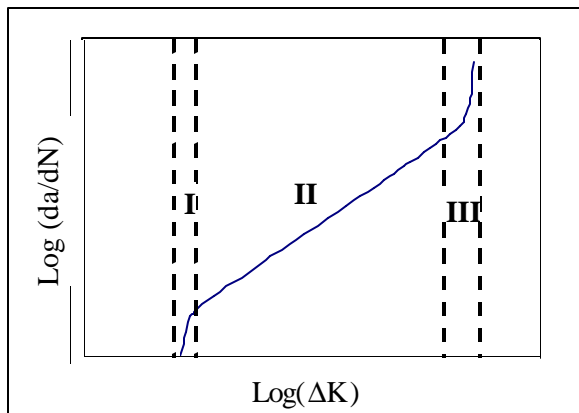


Figure 3.6: Stages of fatigue crack growth

Stage III crack growth is of little engineering significance where the fatigue life is relatively long, because it does not significantly influence the total fatigue life. The next significant limit is the material toughness,  $K_{IC}$ , where fracture occurs as discussed earlier.

### 3.4 CONCLUSION

This chapter has given some background to the development of fracture mechanics. The full theory of fracture mechanics includes elastic-plastic fracture (J-integral), but this chapter only covers LEFM.

Although some justification has been provided for the use of LEFM in this chapter, it must ultimately be evaluated against the parameters of the case study. It is shown in later chapters that the stresses in large turbines are far below yield and that the fracture toughness of the material is such that LEFM is appropriate for the case study.

Numerical solution routines, like finite element analysis, are versatile in the calculation of fracture parameters for complex crack problems or where simplified analytical solutions are not available. In the next chapter, the theory in chapter 2 is combined with the expressions in this chapter to show its implementation in finite element analysis.

